ACS APPLIED MATERIALS & INTERFACES

Research Article

www.acsami.org

Graphite-Nanoplatelet-Decorated Polymer Nanofiber with Improved Thermal, Electrical, and Mechanical Properties

Jiefeng Gao, Mingjun Hu, Yucheng Dong, and Robert K. Y. Li*

Department of Physics and Materials Science, City University of Hong Kong, Tat Chee Avenue, Kowloon, Hong Kong

ABSTRACT: Graphite-nanoplatelet (GNP)-decorated polymer nanofiber composites with hierarchical structures were fabricated by the combination of electrospinning and ultrasonication. It was found that GNPs could be well attached or embedded onto the nanofibers when their size was comparable to the nanofiber diameter. X-ray diffraction results indicated that ultrasonic treatment exerted no influence on the carbon crystal layer spacing. Fourier transform infrared spectra and Raman spectroscopy revealed the existence of interfacial interaction between GNPs and polyurethane nanofibers. The prepared nanofiber composite showed enhanced thermal stability and hardness, which originated from uniform dispersion of GNPs as well as strong interaction between GNPs and the nanofibers. The electrical conductivity was significantly improved, derived from the formation of a conductive percolation network in the nanofiber composite. During ultrasonication, cavitation bubbles may be formed in liquid, and microjets and shock waves were created near the GNP surface after collapse of the bubbles. These jets, causing sintering of GNPs, pushed GNPs toward the nanofiber surface at very high speeds. When the fast-moving GNPs hit the nanofiber surface, interfacial collision between GNPs and the nanofibers occurs, the nanofiber may experience partial softening or even melting at the impact sites, and then GNPs could be uniformly anchored onto the nanofibers. This method opens a new door for harvesting GNP-based nanofiber composites with improved material properties.

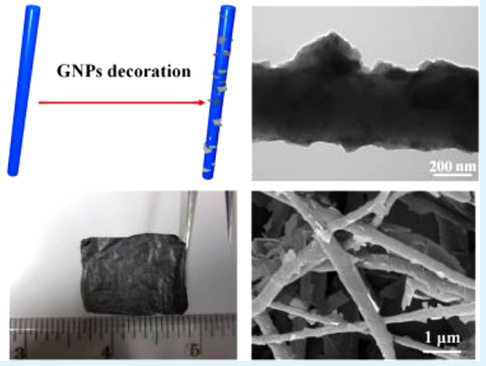

KEYWORDS: *graphite nanoplatelets, ultrasonication, electrospun, nanofibers*

1. INTRODUCTION

Electrospun polymer nanofiber (EPNF) have attracted much attention recently because of their wide applications in many fields such as catalysis, scaffold, and sensors.[1−5] However, the pure polymer nanofibers lack sufficient thermal stability, electrical conductivity, etc., severely limiting their applications. Therefore, nanosized fillers are often incorporated into the nanofiber in order to improve their comprehensive performances. Carbon nanotubes (CNTs) are good candidates because of their superior properties.[6−10] Nevertheless, CNTs are very expensive, and it is thus desirable to seek alternatives. Graphite nanoplatelets (GNPs) seem to be a good choice because they possess excellent thermal, mechanical, and electrical properties and can be obtained at low cost.[11−15] GNPs are usually obtained by so-called "chemical intercalation−hot expansion−ultrasonication"[16−19] and have a large ratio of width to thickness (aspect ratio) and a unique layered structure with nanoscale thickness (from several nanometers to 100 nm).[11,20] GNPs are often dispersed in both thermoplastics and thermosetting polymers for the fabrication of composite materials, which have many potential applications including piezoresistive materials,[21] barrier layers,[22] electromagnetic interference shielding,[23] electrodes,[24] etc. However, to the best of our knowledge, GNPs are seldom employed as fillers in the EPNF, presumably because of their large plane size. On the other hand, good dispersion of GNPs in polymer solution is still a challenge. Mack et al. incorporated GNPs into electrospun polyacrylonitrile nanofibers, and the composite nanofibers displayed a modest increase in thermal stability with increasing weight percent of the GNPs.[25] However, GNPs are easily aggregated in the polymer solution, which is detrimental to the improvement of the material performance and even deteriorates their original quality. In addition, the superior properties, especially the electrical conductivity of GNPs, could not be fully explored when they were wrapped by a layer of insulating polymer.

In fact, GNPs could be located on the nanofiber surface rather than remain inside the nanofibers, which could also improve the properties of the EPNF mat, especially the electrical conductivity and hardness. In our previous work, CNTs were successfully decorated onto the polymer nanofiber surface based on ultrasonition.[26] Here, in this paper, ultrasonication was also employed to induce GNP decoration onto the nanofiber surface, in order to obtain the GNP-anchored nanofiber composite. Ultrasonication serves not only to guarantee good dispersion of GNPs in the solution but also to drive GNP adsorption toward the nanofibers. It is an efficient and energy-saving method because the decoration

Received: April 18, 2013
Accepted: August 2, 2013
Published: August 2, 2013

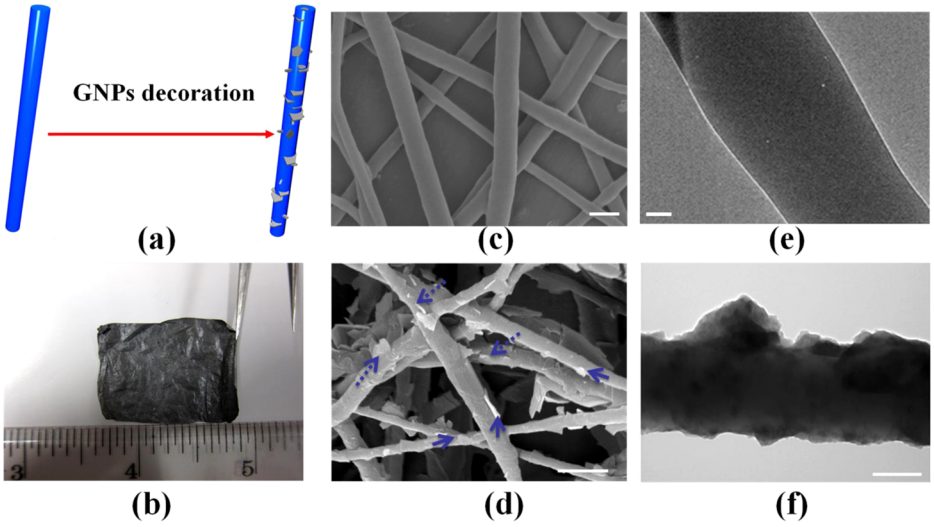

Figure 1. (a) Schematic demonstration of GNP decoration onto electrospun nanofibers. (b) Photograph of the electrospun PU nanofiber mat after GNP decoration. (c and d) SEM and (e and f) TEM images of the PU nanofiber and GNP-anchored PU nanofiber composite. Scale bars: (c and d) 1 μm; (e) 100 nm; (f) 200 nm.

process could be completed within several minutes. Furthermore, it is a surfactant-free method, and good dispersion of GNPs could be preserved on the nanofiber surface during ultrasonication. The interfacial interactions between GNPs and polyurethane (PU) nanofiber were proved by Fourier transform infrared (FTIR) spectra and Raman spectroscopy. The prepared nanofiber composite exhibited enhanced thermal stability and electrical conductivity. GNP decoration also contributed to the large increase in the hardness of the nanofiber film. This approach provides a new strategy for harvesting GNP-based nanofiber composites with improved material properties.

2. EXPERIMENTAL SECTION

2.1. Materials. The graphite intercalated compound (GIC) in the experiment was an expandable sulfuric acid intercalated graphite (code 220-50 N) and was purchased from GrafTech International Ltd. (Parma, OH) with a particle size of about 50 mesh. Here, mesh is a measure of the spacing of the strands of a mesh or grid, defined as the distance between strands for coarse meshes or a number of strands per unit length for fine meshes. In fact, the size for the exfoliated GNPs is about several micrometers. The onset temperature for the release of sulfuric acid for the GIC is 220 °C, and the expansion volume at 600 °C is 200 cm^3/g. The thermoplastic PU (TPU; code Desmopan 385S) was provided by Bayer (Hong Kong, China). The melting point and decomposition temperature for the TPU are 220 and 250 °C, respectively, and the bulk density is 500−700 kg/m^3.[27] *N*,*N*-Dimethylformamide (DMF) was provided by Sigma-Aldrich Corp. (St. Louis, MO) and used as received.

2.2. Preparation of GNPs. The as-received GIC was heated at 600 °C for several seconds to obtain an expanded graphite (EG). In the EG, their dimension in the *c* direction, i.e., the direction perpendicular to the planar direction of the nanoplatelet, was several hundred times that of the original dimension for the GIC. The EG was then dispersed in water and treated using an ultrasonic probe for 6 h to obtain exfoliated GNPs, and the GNP size was about several micrometers. GNPs with sizes of about several hundred nanometers (comparable with the diameter of the electrospun nanofibers) were prepared by extending the ultrasonic time to 24 h. The ultrasonication power is 40% of the maximum power (i.e., 40% of 450 W), and the frequency is 20 kHz.

2.3. Preparation of Electrospun Nanofibers. A certain amount of PU was dissolved in DMF (a good solvent for PU) at a concentration of 13 wt %, and the polymer solution at this concentration possesses a proper viscosity for electrospinning. The PU solution was subjected to mechanical stirring for 8 h before electrospinning, in order to obtain a homegeneous solution. The prepared polymer solution was then loaded into a plastic syringe and fed through a metallic nozzle at a feed rate of 1 mL/h. The applied voltage was 12.5 kV, and the distance from the metallic needle to the surface of the rotating drum was 12.5 cm. A feed rate of 1 mL/h, a voltage of 12.5 kV, and a distance of 12.5 cm could guarantee the formation of long and uniform electrospun nanofibers. The nanofibers were collected on aluminum foil, which was attached to the rotating drum.

2.4. GNP Decoration onto the Electrospun Nanofiber. A total of 25 mg of GNPs was dispersed in 40 mL of deionized water, and then the suspension was subjected to ultrasonication for 1 h. After that, the nanofiber mat was immersed into the GNP solution and experienced ultrasonicaion in an ultrasonic bath for about 3 min. The power and frequency for ultrasonication were 150 W and 20 kHz. The GNP-decorated nanofiber membrane was washed out with deionized water several times, in order to remove the unabsorbed CNTs left on the mat surface. The later experiments demonstrate that this procedure works well. Finally, the gray-black composite mat was dried at 50 °C in an oven for 24 h.

2.5. Characterization. The gold-sputtered GNP-decorated EPNF mat was examined by field-emission scanning electron microscopy (FESEM; FEG JSM6335). Electrospun nanofibers were also directly deposited onto a copper grid for a few seconds during electrospinning for transmission electron microscopy (TEM; Philips FEG CM200) observation. X-ray diffraction (XRD) patterns were recorded on a Philips 220 X'pert diffractometer with Cu Kα radiation (λ = 1.54178 Å). FTIR spectra were recorded on a Perkin-Elmer 100 spectrometer. Raman measurements were performed at room temperature using a Renishaw inVia Raman microscope. The 514 nm radiation from a 20 mW air-cooled argon-ion laser was used as the exciting source. The error is usually within the symbol size and is therefore not depicted for the XRD, Raman, and FTIR curves. Thermogravimetric analysis (TGA) was carried out on a TA Instrument (TGA Q50) system with a scanning range from 25 to 600 °C and a heating rate of 10 °C/min in a nitrogen atmosphere. The electrical conductivity was measured by a four-probe method. We first obtain the resistance of the nanofiber film (R); R is calculated as $R = (V/I)$, which is based on Ohm's law. V and I are the voltage and current, respectively. Then the electrical resistivity could be obtained $R_s = R(S/L)$, where L is the length and S is the cross-sectional area of the nanofiber film. The electrical conductivity is the reciprocal of the resistivity. Nanoindentation tests were conducted

at room temperature using NanoIndenter XP (MTS Cor.) with a triangular diamond indenter at a loading rate of 0.05 mN/s. During a nanoindentation test, the triangular diamond indenter would touch and press down on the thin nanofiber mat at a certain speed, and the hardness could be obtained at each displacement. Three regions in the same sample were measured to obtain the average hardness of the PU nanofiber and GNP-anchored nanofiber mat.

3. RESULTS AND DISCUSSION

GNPs are usually fabricated by a so-called "chemical intercalation−hot expansion−ultrasonication" method. First, the natural graphite flakes are intercalated with a high concentration of acids to prepare the GIC. The obtained GIC experiences rapid expansion at a high temperature to produce EG. The GNPs could finally be obtained by ultrasonic treatment of the EG dispersed in a certain solvent. GNPs used in our experiment possess a layered structure and were prepared through exfoliation of the GIC, and the thickness of the GNPs was about a few tens of nanometers.[27] Figure 1a is a schematic demonstration for ultrasonication-induced GNP decoration onto the nanofiber surface. GNPs are attached or embedded onto the nanofiber surface after ultrasonication. The pure electrospun nanofiber mat was white; however, the nanofiber mat became completely gray-black after GNP decoration (Figure 1b; the minimum unit of the ruler is millimeters), indicating that the nanofibers were successfully decorated by GNPs. The pure PU nanofiber, with a diameter of around 350 nm, possessed a smooth surface, which can be observed from the SEM and TEM images in Figure 1c,e (part e is a magnified TEM image for a single PU nanofiber). However, the nanofiber surface became very rough after GNP decoration, and many GNPs were attached or anchored irregularly onto the nanofiber surface. Some GNPs were tightly attached on the fiber surface (see the solid blue arrows), while others were deeply embedded onto the nanofiber (see the dotted blue arrows), leaving a section of GNPs protruding out of the nanofiber (Figure 1d,f). Here it is proven that GNPs not attached are successfully removed by our preparation. During ultrasonication, cavitation bubbles may be formed in liquid, and the collapse of these bubbles creates a transient temperature of around 5000 K and a pressure of around 1000 atm with a cooling rate above 10^8 K/s.[28,29] Gedanken and co-workers used ultrasound irradiation to coat noble-metal nanocrystals on silica and polystyrene (PS) spheres. The gold nanoparticles were bonded to the silica surface, which was related to the microjets and shock waves generated near the solid surfaces after collapse of the bubbles. These jets, causing sintering of metallic particles, push the nanoparticles toward the silica surface at very high speeds. When these nanoparticles hit the silica surface, they can react with free silanols, or even Si−O−Si bonds, which may lead to the formation of Au−O−Si bonds.[30,31] However, the mechanism of coating nanoparticles on PS spheres might be different because their surfaces and the chemical interactions between the particles are different. PS spheres did not form chemical bonds but rather got coated because of sintering of the particles and/or interparticle collisions between PS and the metal nanoparticles. As a result, the polymer melted or softened, and the metallic particles thus "dissolved" partially in the polymer.[32] Similarly, in our experiment, microjets and shock waves can be generated near the GNP surfaces after collapse of the bubbles during ultrasonication. These jets possessing large energy can push the GNPs toward the nanofiber at high speeds. When the fast-moving GNPs hit the nanofiber surface, interfacial collision between the GNPs and nanofibers occurs. As a consequence, the polymer nanofiber may become softened or even partially melted at the impact sites. Here, the melting or softening is an instantaneous behavior and only happens at the GNP impact site (a very small contact area), and finally GNPs could be decorated onto the nanofibers. Note that the whole polymer nanofiber could not be damaged under an instantaneous impact from the GNPs.

It was reported that ultrasonication could not only exfoliate graphene oxide sheets but also cut them into smaller sheets by the mechanical shock waves and shear forces created by the collapse of cavitating bubbles.[33,34] In our experiment, the GNP size could also be tuned by controlling the ultrasonication time. Figure 2 displays SEM images of anchored nanofiber composites with different GNP sizes. It is found that the GNP size plays an important role in determining the final morphology of the GNP-anchored nanofiber composite. GNPs cannot be well anchored onto the nanofiber surface when their size was much larger than the fiber diameter, as shown in Figure 2a,a′ (the GNP size was more than 1 μm). The large GNPs stack together, occupying the pores between the nanofibers in the mat. However, when the GNP size was comparable to the diameter of the nanofiber (about 350 nm), the separated GNPs were uniformly attached or embedded onto the fiber surface. Fortunately, the pores between the individual nanofibers were preserved even after GNP decoration, which made it possible to take advantage of the large number of interconnected pores in the nanofiber membrane. Fewer GNPs were capable of contacting the nanofiber surface with an increase in their size. On the other hand, the energy causing GNP to keep moving remains the same at constant ultrasonication power. GNPs with larger size correspond to larger weight, and it is understandable that GNPs possessing the same energy have decreased moving velocity if their size and thus their weight increase. As a result, the ultrasonication-induced GNP impacting the nanofiber became weaker.

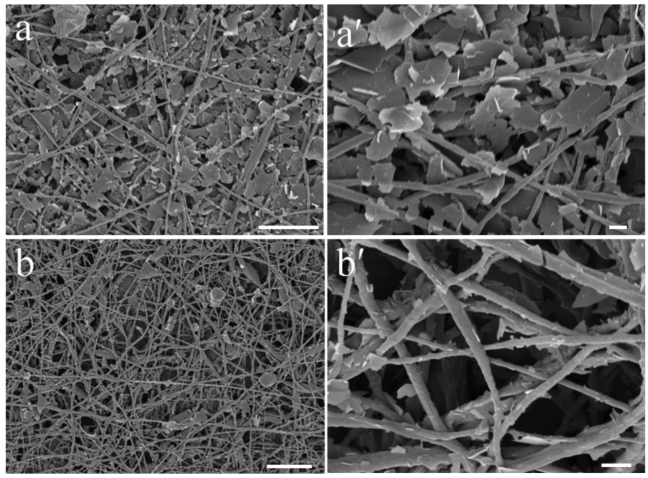

Figure 2. SEM images of the GNP-anchored PU nanofibers with different GNP sizes: (a) larger than 1 μm; (b) several hundred nanometers. (a′ and b′) Magnified images of parts a and b. Scale bars: (a and b) 10 μm; (a′ and b′) 1 μm.

Figure 3 displays the XRD patterns of the PU nanofiber and GNP-anchored PU nanofiber composite. The scattering patterns show the position and intensity of characteristic peaks of crystal or semicrystalline materials, which could

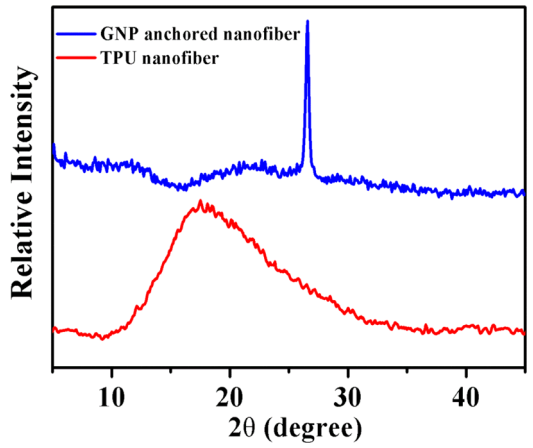

Figure 3. XRD patterns of the PU nanofiber and GNP-anchored PU nanofiber composite.

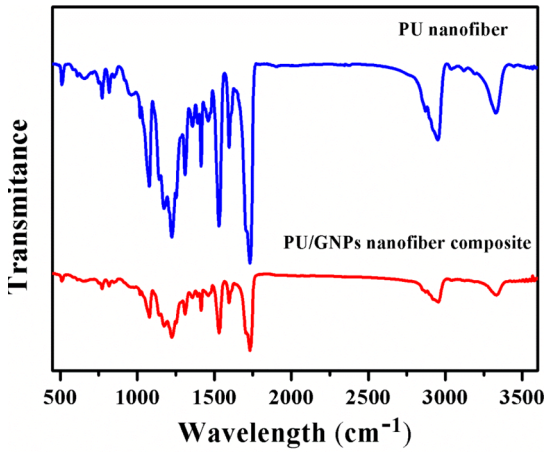

Figure 4. FTIR spectra of the PU nanofiber and GNP-decorated nanofiber composite.

provide information about the size and crystalline structure of the PU nanofiber and GNP-anchored nanofiber composite. In fact, the backgrounds for both TPU and the nanofiber composite were not flat, and there are some small fluctuations, which may come from the instrument error. Fortunately, the main information, i.e., the characteristic peaks, can be clearly observed from the XRD curves. The pure TPU nanofiber shows a very strong broad diffraction peak ranging from 12 to 30° and centered at about 2θ = 19°, referring to the reflection plane of (110) with an interchain spacing of 0.442 nm.[35] This peak also indicates the existence of short-range regular-ordered structures of both hard and soft domains along with a disordered structure of the amorphous phase of the TPU.[36] However, the peak disappears after GNPs were decorated onto the nanofibers. It was reported that the TPU peak became broadened and the intensity decreased with the addition of CNTs. It was assumed that the aggregation/agglomeration dynamics of both soft and hard segments of the TPU matrix was significantly disordered, which might be caused by the presence of strong interfacial interactions between CNTs and the TPU matrix. In addition, the resulting steric hindrance effect of the individual or bundle nanotubes also affected the well-organized accumulation of the soft and hard phases of the TPU matrix.[36] In our experiment, the interaction between GNPs and the nanofiber may have damaged the well short-range microstructural phases of TPU, which finally led to the disappearance of the peak in the GNP-anchored nanofiber composite. For the nanofiber composite, there is a sharp peak around 2θ = 26.6° [(002) diffraction peak of GNPs], which corresponds to a d spacing of 0.335 nm. As mentioned in the Experimental Section, the GNPs were obtained by ultrasonication treatment of the EG, and the EG possesses one major diffraction peak at 26.68°.[27] The sharp (002) peak with almost the same intensity is also found for the GNP-anchored nanfiber composite, indicating that the ultrasonic treatment exerted no influence on the carbon crystal layer spacing.

The interactions between PU and GNPs were studied by FTIR (Figure 4). The FTIR spectra for GNPs could be found elsewhere.[37] For the pure PU nanofiber, the peak at 3328 cm^{-1} is the characteristic N−H stretching band of urethanes, and the two strong vibrations at around 1730 and 1596 cm^{-1} belong to free and hydrogen-bonded carbonyl groups in the urethane linkage (−H−N−COO−). Furthermore, the peak at 1596 cm^{-1} is assigned to N−H in the plane-bending mode, and the peak at 1530 cm^{-1} is associated with the combination of N−H bending and C−H stretching. In addition, the stretching C−O and C−O−C bands are present at 1170 and 1078 cm^{-1}, respectively.[38] No evident changes of the PU bands are observed when GNPs were introduced onto the nanofiber surface except that the position of the N−H stretching band gradually shifts from 3328 cm^{-1} in the pure PU nanofiber to 3332 cm^{-1} in the PU/GNPs nanofiber composites, which might suggest the existence of chemical interactions between the N−H group of PU and the functional groups of GNPs. The interfacial interaction between PU and GNPs is benefical to the reinforcement capacity of GNPs and, consequently, to the final properties of PU/GNPs nanofiber composites.

The possible interactions between GNPs and the PU nanofiber were also investigated by Raman spectroscopy, as shown in Figure 5. PU's characteristic vibration bands,

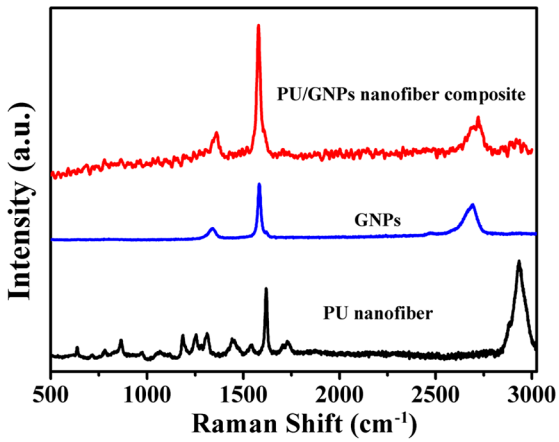

Figure 5. Raman spectra of GNPs, the neat PU nanofiber, and the GNP-decorated nanofiber composite.

including δ(C−H) at 1445 cm^{-1}, ν(C═C) at 1620 cm^{-1}, ν(C═O) at 1734 cm^{-1}, and $\nu(CH_2)$ at 2932 cm^{-1}, could be observed.[38,39] The average bond enthalpies for C−C, C−H, C═C, C═O, and O−H are 438, 413, 614, 799, and 463 kJ/mol. For GNPs, three typical peaks at about 1340, 1580, and 2692 cm^{-1} were present, corresponding to the D, G, and 2D bands, which are the signatures of graphite-like structure.[40,41] As is known, the D band is related to the defects introduced

dx.doi.org/10.1021/am401420k | ACS Appl. Mater. Interfaces 2013, 5, 7758−7764

into the structure, whereas the G and 2D peaks correspond to the in-plane C−C bond stretching in GNPs. It was found that the intensity of the D to G peak is very small (I_D/I_G = 0.15), indicating a small amount of defects present in the as-prepared GNPs. It was worth noting that the characteristic polymer bands become less obvious and even disappear after GNP deocration to the PU nanofiber surface. On the other hand, the characteristic D and 2D bands are up-shifted from 1340 and 2692 to 1360 and 2719 cm^{-1} by 20 and 27 cm^{-1}, indicating interactions between the PU nanofiber and GNPs that may be due to interfacial stress transfer.[42] We do not know the exact reason in terms of the small signal fluctuation for the nanofiber composite, but the position and intensity of the characteristic can be clearly identified in spite of the small signal fluctuation. The Raman spectroscopy provides some sensitive information about the chemical interactions between GNPs and TPU caused by the presence of carboxylic and hydroxy groups and/or additional disorder-related defects on GNPs. These interactions may be responsible for the improved material properties, which will be discussed in the following sections.

The thermal stability of the GNP-decorated nanofiber composite was investigated by TGA, which can be observed in Figure 6. The weight ratios of the residual for the PU

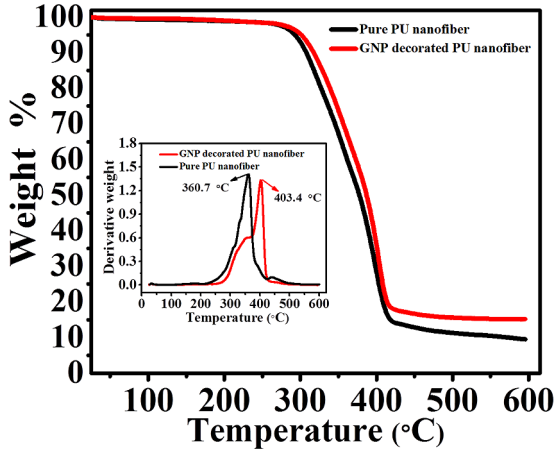

Figure 6. TGA curves for the pure PU nanofiber and GNP-anchored PU nanofiber.

nanofiber mat and GNP-anchored PU nanofiber composite mat after thermal degradation are about 9.5% and 14.1% respectively. Here, we assume that the weights for GNPs absorbed onto the nanofibers and the pure polymer nanofibers are m_g and m_p, respectively. The total weight of the nanofiber composite is $m_t = m_g + m_p$. On the basis of the TGA results, $14.1\%m_t = m_g + 9.5\%m_p$, finally the weight ratio of GNPs absorbed onto the nanofiber composite, i.e., $m_g/m_t \times 100\%$, is calculated as about 5.1%. It is also found that the TGA curve for the nanofiber composite shifted toward the zone of high temperature, suggesting that the thermal stability of the PU nanofiber membrane was enhanced. Moreover, the temperature for the maximum weight loss rate increased from 360.7 to 403.4 °C. The improved thermal stability might originate from good dispersion of the GNPs as well as strong interaction between the GNPs and nanofibers. During ultrasonication, the GNPs could be separated from each other, and the individual GNPs could be uniformly decorated onto the nanofiber surface, which could be observed from the SEM image in Figure 1d. On the other hand, GNPs hit the nanofiber strongly under ultrasonication, causing the softening or even partial melting of the TPU at the impact sites, and GNPs could thus adhere to the nanofiber tightly, leading to the strong interaction between them.

To improve the conductivity and decrease the percolation threshold, conductive fillers such as carbon black, CNTs, and graphene were selectively located on the interface of the polymer matrix particles instead of being randomly distributed in the whole system, i.e., construction of a segregated structure in the composite.[43−46] In a microfibrillar blend composite, when the content of the conductive filler was beyond the maximun packing fraction (φ_{max}), the filler could migrate to the surface of the microfibrils and thus a continuously conductive network was built in the composite.[47] To reach φ_{max}, a large amount of conductive filler must be incorporated into the microfibrils, and most of them just stayed inside the microfibrils, contributing little to the conductivity. Therefore, the conductive fillers are often controlled to be distributed on the surface of the microfibrils, in order to obtain the conductive polymer composite with a low percolation threshold. It was reported that the conductive pathway was formed when the CNTs were selectively located on the microfibrillar surface.[48] In our experiment, the conductive filler, namely, the GNPs, was designed to be located on the fiber surface, and the conductivity of the GNP-decorated nanofiber mat was about 3.8×10^{-1} S/m, exhibiting a good electrical property (the conductivity of the pure PU nanofiber mat is 10^{-12} S/m). Electrospun nanofibers became conductive elements after GNP decoration, and the conductive nanofibers with high aspect ratios were beneficial to formation of the conductive network.[49] In addition, the conductive pathway had low junction resistance because of the presence of many contact points of GNPs. High conductivity cannot be achieved if GNPs were incorporated inside nanofibers because there was a layer of nearly pure polymer on the nanofiber surface, which offered resistance to electron transportation. Therefore, ultrasonication-induced GNP decoration is a promising technique to improve the electrical performance of the nanofiber membrane.

Nanoindentation was carried out to measure the hardness of the nanofiber mat, which is shown in Figure 7. Displacement

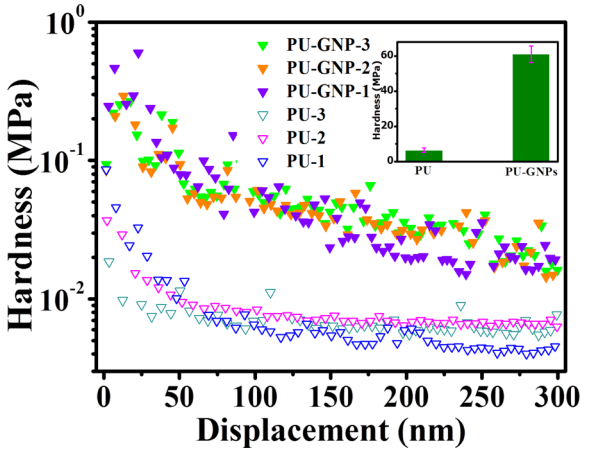

Figure 7. Hardness of the PU nanofiber and GNP-decorated nanofiber composite as a function of the displacement. The GNP content in the nanofiber composite as derived from our TGA is 5.1 wt %. Three different positions in the nanofiber mats were chosen to measure the hardness, and the inset displays the average hardness for the two samples.

dx.doi.org/10.1021/am401420k | ACS Appl. Mater. Interfaces 2013, 5, 7758−7764

here refers to the distance of the indenter movement, which can be accurately controlled in the range of subnanometers, and the hardness could be obtained at each displacement. It could be observed that the hardness decreases quickly and then gradually reaches an equilibrium value. The hardness of GNP-decorated nanofibers (60 MPa) was more than 8 times higher than that of the pure nanofiber (7 MPa). The significantly improved hardness might result from good dispersion of the GNPs on the nanofiber surface as well as strong interaction between the GNPs and nanofibers. Generally, dispersion of nanofillers such as CNTs should be very good in the polymer matrix, in order to realize the enhancement of most of the nanocomposite's properties;[50] otherwise, the fillers tend to aggregate to form large agglomerates, and bad dispersion would probably deteriorate the comprehensive properties of the materials. To this end, a surfactant is often utilized to assist their dispersion. However, it was reported that the use of dispersant could lower Young's modulus of the electrospun fibers.[51] On the other hand, the interfacial bonding between the filler and polymer matrix was very important for improving the mechanical properties of the composite fiber because the load can effectively transfer to the fillers if good interfacial interaction is achieved.[52] In our experiment, GNP adsorption was a surfactant-free process, and the well-dispersed GNPs benefiting from ultrasonication were inherited after the adsorption process and uniformly anchored onto the nanofibers, which can be observed from the SEM image in Figure 1d,f. GNPs hit the nanofiber strongly during ultrasonication adsorption, causing the softening of TPU at the impact sites; therefore, GNPs could be attached onto the nanofiber tightly, leading to strong interaction between the CNTs and nanofibers. Moreover, the oxygen-containing groups on the GNPs and amino group of PU promoted the interfacial interaction, which was illustrated by FITR and Raman spectroscopy. As a result, the TPU nanofibers were wrapped by the rigid GNPs, leading to a great improvement of the hardness.

4. CONCLUSION

In summary, we have proposed a facile method, i.e., the ultrasonication-induced uniform decoration of GNPs onto the polymer nanofiber surface, to obtain the GNP-anchored nanofiber composite. Ultrasonication serves not only to guarantee good dispersion of GNPs in the solution but also to drive GNP adsorption toward the nanofiber. When the GNP size was comparable to the nanofiber diameter, GNPs could be well attached or embedded onto the nanofiber. XRD results indicated that ultrasonic treatment exerted no influence on the carbon crystal layer spacing. FTIR and Raman spectroscopy revealed the existence of interfacial interaction between the GNPs and PU nanofibers. The GNP-anchored nanofiber composite showed enhanced thermal stability and hardness, which originated from the uniform dispersion of GNPs and strong interaction between the GNPs and polymer nanofiber. The conductivity was significantly improved because of formation of the conductive network as well as the low junction resistance in the composite. This method opens a new door for harvesting GNP-based nanofiber composite with improved material properties.

AUTHOR INFORMATION

Corresponding Author

*E-mail: aprkyl@cityu.edu.hk.

Notes

The authors declare no competing financial interest.

ACKNOWLEDGMENTS

This work is supported by a CityU SRG grant (Project 7002752).

REFERENCES

(1) Huang, Z. M.; Zhang, Y. Z.; Kotaki, M.; Ramakrishna, S. *Compos. Sci. Technol.* **2003**, *63*, 2223−2253.
(2) Li, D.; Xia, Y. N. *Adv. Mater.* **2004**, *16*, 1151−1170.
(3) Xu, X. F.; Wang, C.; Wei, Y. *Small* **2009**, *5*, 2349−2370.
(4) Agarwa, S.; Greiner, A.; Wendorf, J. H. *Adv. Funct. Mater.* **2009**, *19*, 1−17.
(5) Reneker, D. H.; Yarin, A. L. *Polymer* **2008**, *49*, 2387−2425.
(6) Havel, M.; Behler, K.; Korneva, G.; Gogotsi, Y. *Adv. Funct. Mater.* **2008**, *18*, 2322−2327.
(7) Ge, J. J.; Hou, H.; Li, Q.; Graham, M. J.; Greiner, A.; Reneker, D. H.; Harris, F. W.; Cheng, S. Z. D. *J. Am. Chem. Soc.* **2004**, *126*, 15754−15761.
(8) Sui, X. M.; Giordani, S.; Prato, M.; Wagner, H. D. *Appl. Phys. Lett.* **2009**, *95*, 233113.
(9) Naebe, M.; Lin, T.; Staiger, M. P.; Dai, L. M.; Wang, X. G. *Nanotechnology* **2008**, *19*, 305702.
(10) Sundaray, B.; Subramanian, V.; Natarajan, T. S.; Krishnamurthy, K. *Appl. Phys. Lett.* **2006**, *88*, 143114.
(11) Sengupta, R.; Bhattacharya, M.; Bandyopadhyay, S.; Bhowmick, A. K. *Prog. Polym. Sci.* **2011**, *36*, 638−670.
(12) Raza, M. A.; Westwood, A.; Brown, A.; Hondow, N.; Stirling, C. *Carbon* **2011**, *49*, 4269−4279.
(13) Debelak, B.; Lafdi, K. *Carbon* **2007**, *45*, 1727−1734.
(14) Ganguli, S.; Roy, A. K.; Anderson, D. P. *Carbon* **2008**, *46*, 806−817.
(15) Hung, M. T.; Choi, O.; Ju, Y. S.; Hahn, H. T. *Appl. Phys. Lett.* **2006**, *89*, 023117.
(16) Zhao, Y. F.; Xiao, M.; Wang, S. J.; Ge, X. C.; Meng, Y. Z. *Compos. Sci. Technol.* **2007**, *67*, 2528−2534.
(17) Zheng, W. G.; Wong, S. C.; Sue, H. J. *Polymer* **2002**, *43*, 6767−6773.
(18) Li, J.; Kim, J. K.; Sham, M. L. *Scr. Mater.* **2005**, *53*, 235−240.
(19) He, F.; Lau, S. T.; Chan, H. L. W.; Fan, J. T. *Adv. Mater.* **2009**, *21*, 710−715.
(20) Jang, B. Z.; Zhamu, A. *J. Mater. Sci.* **2008**, *43*, 5092−5101.
(21) Lu, J.; Weng, W.; Chen, X.; Wu, D.; Wu, C.; Chen, G. *Adv. Funct. Mater.* **2005**, *15*, 1358−1363.
(22) Kalaitzidou, K.; Fukushima, H.; Drzal, L. T. *Carbon* **2007**, *45*, 1446−1452.
(23) Liang, J.; Wang, Y.; Huang, Y.; Ma, Y.; Liu, Z.; Cai, J.; Zhang, C.; Gao, H.; Chen, Y. *Carbon* **2009**, *47*, 922−925.
(24) Kujawski, M.; Pearse, J. D.; Smela, E. *Carbon* **2010**, *48*, 2409−2417.
(25) Mack, J. J.; Viculis, L. M.; Ali, A.; Luoh, R.; Yang, G.; Hahn, H. T.; Ko, F. K.; Kaner, R. B. *Adv. Mater.* **2005**, *17*, 77−80.
(26) Gao, J. F.; Hu, M. J.; Li, R. K. Y. *J. Mater. Chem.* **2012**, *22*, 10867−10872.
(27) Quan, H.; Zhang, B. Q.; Zhao, Q.; Yuen, R. K. K.; Li, R. K. Y. *Composites, Part A* **2009**, *40*, 1506−1513.
(28) Lord Rayleigh, O. M. *Philos. Mag.* **1917**, *34*, 94−98.
(29) Flint, E. B.; Suslick, K. S. *Science* **1991**, *253*, 1397−1399.
(30) Pol, V. G.; Gedanken, A.; Calderon-Moreno, J. *Chem. Mater.* **2003**, *15*, 1111−1118.
(31) Sivakumar, M.; Gedanken, A. *Ultrason. Sonochem.* **2004**, *11*, 373−378.
(32) Pol, V. G.; Grisaru, H.; Gedanken, A. *Langmuir* **2005**, *21*, 3635−3640.
(33) Khan, U.; Porwal, H.; O'Neill, A.; Nawaz, K.; May, P.; Coleman, J. N. *Langmuir* **2011**, *27*, 9077−9082.

(34) Qi, G. Q.; Cao, J.; Bao, R. Y.; Liu, Z. Y.; Yang, W.; Xie, B. H.; Yang, M. B. *J. Mater. Chem. A* **2013**, *1*, 3163−3170.
(35) Bian, J.; Lin, H. L.; He, F. X.; Wei, X. W.; Chang, I. T.; Sancaktar, E. *Composites, Part A* **2013**, *47*, 72−82.
(36) Barick, A. K.; Tripathy, D. K. *Mater. Sci. Eng., B* **2011**, *176*, 1435−1447.
(37) Quan H. Preparation and properties of graphite nanoplatelets hybrid polymer composite. Ph.D. Thesis, City University of Hong Kong, Hong Kong, China, 2009. Accessed Aug 1, 2013, http://lib.cityu.edu.hk/record=b2374833.
(38) Menes, O.; Cano, M.; Benedito, A.; Giménez, E.; Castell, P.; Maser, W. K.; Benito, A. M. *Compos. Sci. Technol.* **2012**, *72*, 1595−1601.
(39) Chen, X. H.; Chen, X. J.; Lin, M.; Zhong, W. B.; Chen, X. H.; Chen, Z. H. *Macromol. Chem. Phys.* **2007**, *208*, 964−972.
(40) Ferrari, A. C.; Meyer, J. C.; Scardaci, V.; Casiraghi, C.; Lazzeri, M.; Piscanec, S.; Jiang, D.; Novoselov, K. S.; Roth, S.; Geim, A. K. *Phys. Rev. Lett.* **2006**, *97*, 187−401.
(41) Dresselhaus, M. S.; Jorio, A.; Hofmann, M.; Dresselhaus, G.; Saito, R. *Nano Lett.* **2010**, *10*, 751−758.
(42) Huang, Y. Y.; Ahir, S. V.; Terentjev, E. M. *Phys. Rev. B* **2006**, *73*, 125422−125430.
(43) Gao, J. F.; Li, Z. M.; Meng, Q. J.; Yang, Q. *Mater. Lett.* **2008**, *62*, 3530−3532.
(44) Zhang, C.; Ma, C. A.; Wang, P.; Sumita, M. *Carbon* **2005**, *43*, 2544−2553.
(45) Ju, S. A.; Kim, K.; Kim, J. H.; Lee, S. S. *ACS Appl. Mater. Interfaces* **2011**, *3*, 2904−2911.
(46) Pang, H.; Bao, Y.; Xu, L.; Yan, D. X.; Zhang, W. Q.; Wang, J. H.; Li, Z. M. *J. Mater. Chem. A* **2013**, *1*, 4177−4181.
(47) Dai, K.; Xu, X. B.; Li, Z. M. *Polymer* **2007**, *48*, 849−859.
(48) Gao, J. F.; Yan, D. Y.; Yuan, B.; Huang, H. D.; Li, Z. M. *Compos. Sci. Technol.* **2010**, *70*, 1973−1979.
(49) Wu, H.; Hu, L. B.; Rowell, M. W.; Kong, D.; Cha, J. J.; McDonough, J. R.; Zhu, J.; Yang, Y.; McGehee, M. D.; Cui, Y. *Nano Lett.* **2010**, *10*, 4242−4248.
(50) Bikiaris, D.; Vassiliou, A.; Chrissafis, K.; Paraslevopoulos, K. M.; Jannakoudakis, A.; Docoslis, A. *Polym. Degrad. Stab.* **2008**, *93*, 952−967.
(51) Wang, W.; Ciselli, P.; Kuznetsov, E.; Peijs, T.; Barber, A. H. *Philos. Trans. R. Soc., A* **2008**, *366*, 1613−1626.
(52) Saeed, K.; Park, S. Y.; Haider, S.; Baek, J. B. *Nanoscale Res. Lett.* **2009**, *4*, 39−46.